Materials Research. 2023; 26:e20230017
DOI: https://doi.org/10.1590/1980-5373-MR-2023-0017

Obtention of Hard Coating Using Electrochemical Process in Aluminum-Silicon Alloys for Automotive Vehicles

P.R.C. Silva[a]*, *M.A. Colosio*[a], *M.T.D. Orlando*[b], *J.L. Rossi*[a]

[a]*Instituto de Pesquisas Energéticas e Nucleares (IPEN), Centro de Ciência e Tecnologia de Materiais (CNEN/SP), Av. Professor Lineu Prestes, 2242, 05508-000, São Paulo, SP, Brasil.*

[b]*Universidade Federal do Espirito Santo (UFES), Av. Fernando Ferrari, 514, Goiabeiras, Vitória, ES. Brasil.*

Received: January 09, 2023; Revised: May 22, 2023; Accepted July 05, 2023

Automotive industry is searching for new ways to improve vehicles' energy efficiency through mass reduction, using aluminum alloys. This change requires a surface protection to extend the life cycle of the components and aluminum anodization is the most used solution. This research is focused on the intake and exhaust ducts' surfaces of aluminum internal combustion engines cylinder head, which are subject to chemical agents and temperature variation. To extend the working life of this component it is necessary to obtain a covering protective layer. The process targeted the anodization of an internal surface of a much larger part of a cast aluminum-silicon alloy cylinder head. The anodization was obtained using a H_2SO_4 solution (184 $g.L^{-1}$) and a DC voltage starting at 20 V. The Al_2O_3 layer obtained, inside the cylinder head´s ducts, has an average thickness of 120 µm in accordance with the proposal of providing a suitable surface protection.

Keywords*: anodization, aluminum, surface protection, thermal resistance.*

1. Introduction

The aluminum anodization processes related to the formation of protective alumina (Al_2O_3) layers, were first used on 1854. Ever since, new aluminum alloys were developed and this electrochemical process is widely used for most surface protection applications. The automotive industry is searching for new ways to improve vehicles' energy efficiency and the main initiative is mass reduction. The replacement of heavy materials is crucial and the aluminum alloys are being widely used as a substitute. Several steel parts are being replaced by cast aluminum parts on all major subsystems such as engines, suspension, body structure and others. This material replacement in many cases requires a surface protection to extend the life cycle of the components and aluminum anodization is the most used solution.

Internal combustion engines are subject to a huge amount of heat and require a large cooling system to keep the operational temperature under control. The combustion heat is transferred directly to the aluminum alloy on the cylinders' heads combustion chambers and exhaust ducts inside the cylinder head. To increase the energy efficiency, this heat transfer needs to be lowered as much as possible. Cylinder heads are, in almost every engine, produced with cast aluminum alloys from the AA 3XX series, which has silicon as its most significant alloy element. Al-Si alloys are widely used in castings due to their low melting temperature, high fluidity and low trend to show solidification cracks, and high mechanical strength after heat treatment[1-5].

The anodization process requires an electrical direct or alternate current power source, an electrolyte solution, a cathode (a conductive material that is inert in contact with the electrolyte), and the anode, which is the part from which the anodic oxide will grow[6-12].

When the part and the cathode are both in direct contact with the electrolyte, an electrochemical process occurs when an electric current is forced in the system promoting the transformation of the metallic aluminum into an oxide layer (Al_2O_3), according to Equation 1. This oxide layer grows from the anode surface in a so-called duplex structure composed by a barrier layer and a porous layer. This structure is shown on Figure 1.

$$2Al + 3H_2O \rightarrow Al_2O_3 + 6H^+ + 6e^- \quad (1)$$

After the anodization process, there is an additional stage required do close the pores, called sealing. The sealing process can be done using steam, hot water or salt solutions[6,9,12-14]. This additional process promotes the closing of all pores, increases the oxide layer corrosion resistance and reduces the thermal cracking, and any chemical retention inside the pores[14].

This research´s aim was to obtain an aluminum oxide layer performing a hard anodization on the inner surfaces of the exhaust ducts of a cylinder head. The oxide layer should achieve a compact structure with thicknesses exceeding 100 µm, large cells and the smallest possible pores diameters. Several anodization runs were required to adjust the process parameters to obtain the target configuration. This layer is meant to reduce the heat transfer from the exhaust gas to the cylinder head body, causing a reduction of the engine´s cooling requirements and therefore, the cooling system´s mass. The application is shown on Figures 2 and 3.

*e-mail: paulo.costinhas@hotmail.com

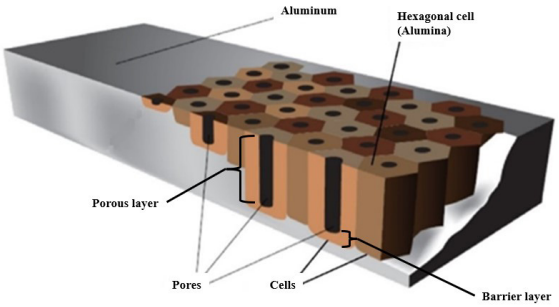

Figure 1. Aluminum oxide layer hexagonal order structure showing Al_2O_3 cells with both barrier layer and porous layer.
Source: Castro and Sillos[13] (adapted). Reprint with permission (Castro and Sillos[13]) copyright 2012 SurTec.

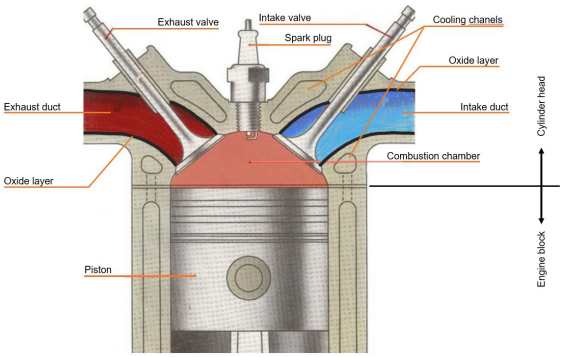

Figure 2. Internal combustion engines schematics showing the main components such as piston, piston rings, valves, spark plug and the target surfaces for protection, the intake and exhaust ducts.
Source: http://www.autoentusiastasclassic.com.br/2010/07/album-de-motores.html?m=1. Reprint with permission. (Adapted)

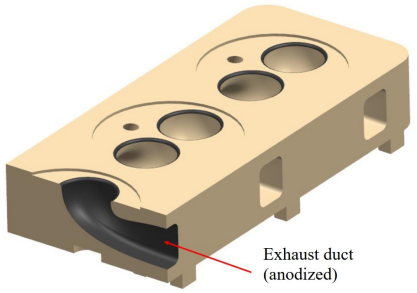

Figure 3. Internal combustion engines cylinder head section, showing several ducts, valve seats and the anodized inner surface area (gray contrast) of an exhaust duct.
Source: author

Oxide layers on Al-Si alloys do not present a regular thickness due to silicon particles that act as a physical barrier to the oxide growth. Given this scenario, experimental parameters were stablished to be pursued as a goal. They were the obtention of the most regular possible thickness layer and an average thickness value of 120 μm.

2. Materials and Methods

This topic addresses the anodization process development stages including materials, parameters, fixtures and equipment.

2.1. Specimen

A regular production cylinder head cast with a modified AA 380 alloy, developed by General Motors - GM (nominal chemical composition: Al-7.5 Si-3.5 Cu mass%), was manufactured using permanent mold casting. The component alloy composition and a comparison with the standard AA 380 alloy can be seen on Table 1. Prior to anodizing, the samples and ducts' surfaces were cleansed, stripped in a 10 mass % sodium hydroxide plus 3 mass % sodium fluoride solutions for 10 minutes, rinsed in demineralized water and air-dried. The EDS measured phase's mass percentage values can be seen on Table 1.

2.2. Anodic oxidation

The ducts' surfaces were anodized at an electric voltage from 20 V to 40 V (DC), with a constant current density of 4.2 $A.dm^{-2}$ (until reaching 40 V) in a 184 $g.L^{-1}$ H_2SO_4 solution at 4 ºC to 6 ºC for 480 minutes. To reach the required process temperature the electrolyte was cooled on an external cooling unit and pumped directly through the cylinder head ducts. It was necessary to develop a fixture that allowed this cooled electrolyte flow to reach only the anodization targeted surfaces. The electrolyte laminar flow of 5 $L.min^{-1}$ improved temperature distribution throughout the target area during the anodization process. A sketch of the fixture schematics is shown on Figure 4.

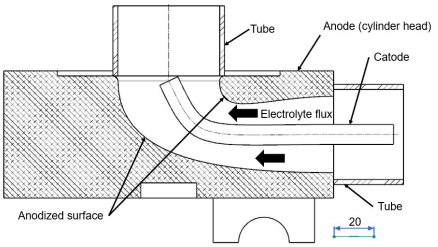

Figure 4. Anodization process fixture sketch showing a section of a cylinder head exhaust duct, tubes to pump the electrolyte through the duct and the cathode bar positioned inside the duct.
Source: author

Table 1. Aluminum alloys composition (mass %) comparison between standard AA380 alloy, GM specified standard and semi-quantitative chemical analysis using energy dispersive spectroscopy (EDS).

Alloys	Si	Cu	Fe	Mg	Mn	Zn	Ni	Sn	Others
AA 380	7.5-9.5	3.0-4.0	< 1.3	< 0.1	< 0.5	< 3.0	< 0.5	< 0.35	< 0.5
GM (specs)	6.5-8.0	3.0-4.0	< 0.8	0.3-0.6	0.2-0.5	< 0.8	< 0.3	< 0.15	< 0.15
GM (EDS)	12.3	2.4	0.6	0.2	0.4	n.	n.	n.	n.

n. = not detected

After anodizing, the part was thoroughly rinsed in demineralized water at 10 °C, followed by a rest time to get back to room temperature and then submersed in hot water at 30 °C, then heated to 98 ºC and kept for 120 minutes to promote the pores sealing, followed by air drying at room temperature.

The anodization results (i.e. oxide layer porosity, thickness and regularity) are driven by the process parameters as electric voltage, current density, electrolyte temperature and process time. The development stages required several steps with parameters adjustments before reaching a set of parameters that resulted on an obtained oxide layer with a sufficient thickness average and uniformity according to the stablished values. It started with the anodization of samples in a format of blocks that were taken from a cylinder head cast with dimensions of 10x10x5 mm^3 and ended with the localized anodization of a full cylinder head exhaust ducts. The process parameters' developments are summarized on Table 2. The cathodes were prepared according to the specimens' geometry, i.e., for the block samples the cathodes were two 100x100x3 mm^3 aluminum 99% pure plates positioned on each opposite side of the sample in a standard beaker. For the cylinder head ducts, the cathodes were prepared using cylindrical bars of a 99% pure aluminum, with a nominal diameter of 15 mm and 10 mm according to the available space inside the ducts.

The anodization parameters (up to stage 9) were determined on a cast only cylinder head #1. After this, a new machined functional regular production cylinder head #2 had its four exhaust ducts anodized and was submitted to a usage test on a dynamometer at GM. This test simulates an actual everyday usage of an engine for approximately 85,000 km[15], to assure the proper operation of the engine while testing the oxide layer resistance and durability when submitted to an actual thermal cycling of an internal combustion engine for a long usage period.

As far as the research through the literature and the patent databases could find, this developed process is unique and limits the required resources for the target surface anodization. It allows a localized anodization of an internal surface on an Al-Si cast alloy obtaining a surface protection just where it is needed[16].

3. Results and Discussion

The oxide layers obtained on each stage are shown on Figures 5 to 13 and a detailed description of the incremental changes made during the anodization process parameters optimization is shown after each stage.

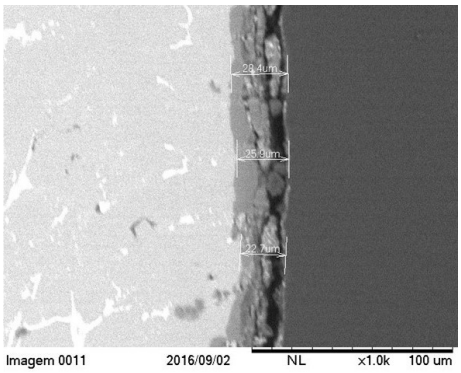

Figure 5. Oxide layer thickness obtained with process parameters of stage #1.
Source: author

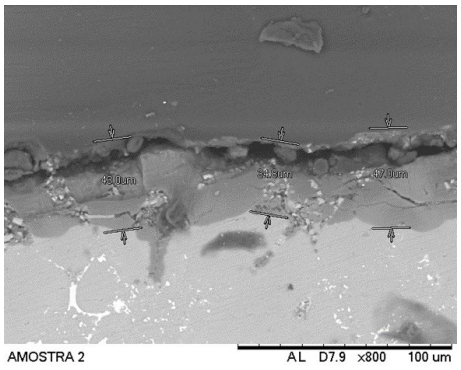

Figure 6. Oxide layer thickness obtained with process parameters of stage #2.
Source: author

Table 2. Anodization parameters used on each development stage until reaching the target thickness average value and uniformity. The used electrolyte throughout the stages was H_2SO_4 184 $g.L^{-1}$.

	Anode	Cathode	E_v (V)	i ($A.dm^{-2}$)	Process temp. (ºC)	Process time (min.)	Sealing temp. (ºC)	Sealing time (min.)
Stage 1	Sample	Plate	20	-	15	120	70	120
Stage 2	Sample	Plate	20	-	10	240	70	120
Stage 3	Sample	plate	20-40	4.2	10	480	70	120
Stage 4	Sample	Plate	20-40	4.2	2-5	480	98	120
Stage 5	Sample	Plate	20-40	4.2	0-2	480	98	120
Stage 6	Duct #1	Bar	20-40	4.2	4-6	480	98	120
Stage 7	Duct #2	Bar	20-40	4.2	4-6	480	98	120
Stage 8	Duct #3	Bar	20-40	4.2	4-6	480	98	120
Stage 9	Duct #4	Bar	20-40	4.2	4-6	480	98	120
Stage 10	Cyl. head #2 ducts #1-4	Bar	20-40	4.2	0-2	480	98	120

E_v = electric voltage; i = current density; - = not measured

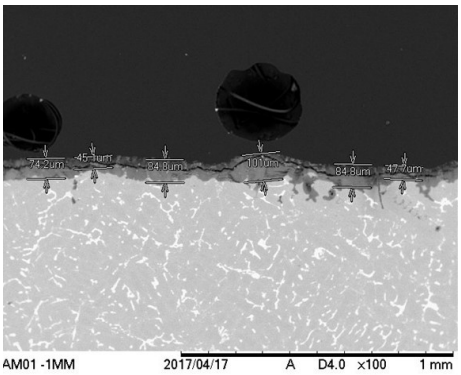

Figure 7. Oxide layer thickness obtained with process parameters of stage #3.
Source: author

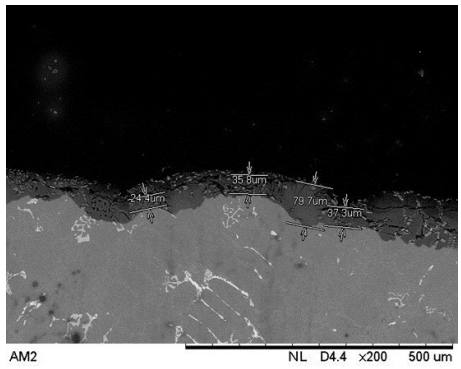

Figure 8. Oxide layer thickness obtained with process parameters of stage #4.
Source: author

On stage #1 the anodization parameters used were taken from Tajima[6]. The obtained oxide layer had an average thickness of 25 µm that did not achieve the target thickness and showed that silicon indeed impairs oxide growth over the entire surface. The oxide layer had cracks in almost all of its extension, see Figure 5. On stage #2 the temperature was lowered to get a more compact porous layer and process time was increased to get a thicker layer. A small increase of 15 µm to 20 µm on the thickness was observed but the cracks were still present, see Figure 6.

On stage #3 the process time was further increased to achieve a thicker layer. The electric voltage varied to maintain a constant current density that allows a more consistent layer growth. This was done until the power source limit of 40 V was achieved. A significant increase on the thickness was observed, achieving an average of 75 µm but the cracks were still present, see Figure 7. On stage #4 the process temperature was lowered and the electric voltage varied to maintain a constant current density. This was done until the power source limit of 40 V was achieved. Also, the sealing temperature was raised to 98 ºC. No significant increase on the thickness was observed and the cracks were still present, see Figure 8.

On stage #5 the process temperature was lowered to the recommended values for the "hard anodization" type, that are -2 ºC to +2 ºC. It was necessary to add an additional cooling unit to achieve 0 ºC on the electrolyte temperature during the anodization process. Another small increase on the thickness was observed and also significant reductions on the cracks extension, due to a more compact oxide layer, see Figure 9. On stage #6 the anodization of an entire duct inner surface was performed. Process parameters of stage #5 were kept, with the exception of temperature. The cooling units were not suitable to the size of the entire cylinder head. There was an increase of 4 ºC on the process temperature. The oxide layer average thickness was maintained, and the cracks extension was still an issue, see Figure 10.

On stages #7 and #8 the anodization was performed on ducts #2 and #3 and the results were similar to the first duct, see Figures 11 and 12.

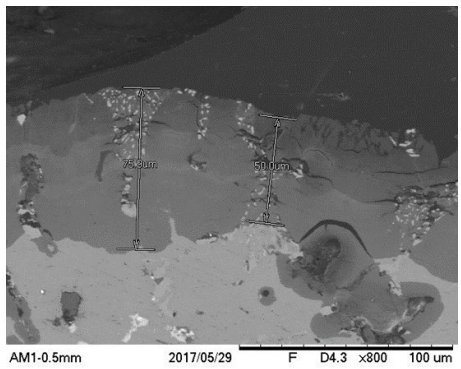

Figure 9. Oxide layer thickness obtained with process parameters of stage #5.

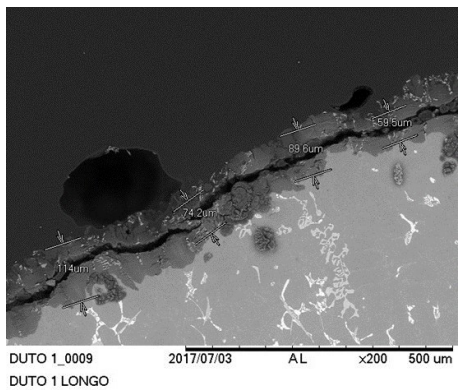

Figure 10. Oxide layer thickness obtained with process parameters of stage #6.
Source: author

After stage #8 a series of considerations took place to investigate the reasons behind the cracks. It was observed that the inlay process, or resin mounting, could be the cause. This is performed on a device that applies high pressure over the sample, immersed on a phenolic resin powder.

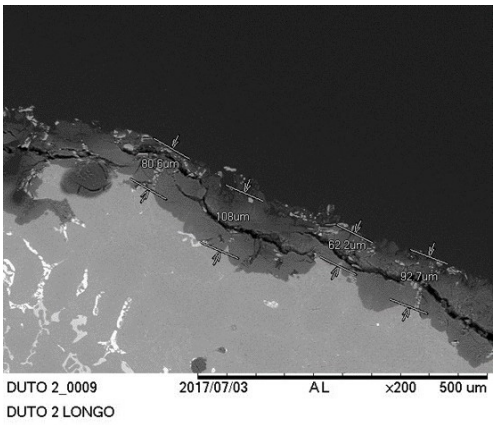

Figure 11. Oxide layer thickness obtained with process parameters of stage #7.
Source: author

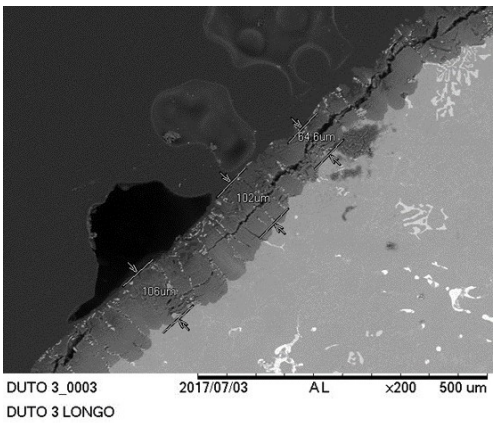

Figure 12. Oxide layer thickness obtained with process parameters of stage #8.
Source: author

The pressurized content was heated up to 150 ºC for 8 minutes and then cooled with water. The resin powder under high pressure and temperature molds into a solid block containing the part sample inside it. The resin bonds to the sample surfaces during the molding process and the assessment was that the resin contraction during the cooling step was pulling the oxide layer and provoking cracks The next stage samples were protected with an aluminum foil prior to the inlay process and the resin cooling time was increased. Figure 13 shows the resin, the sample with an oxide layer, the aluminum foil in the middle, and a distance between the contracted resin and the sample surface that did not present cracks.

On stage #9 the anodization was performed on duct #4. The thickness results were similar to the first three, without the occurrence of cracks. The stage #9 surface appearance after the anodization process is shown on Figure 14. The uniform oxide layer covers the entire surface of the exhaust duct.

After the anodization parameters' optimization stages, the electrolyte cooling units were optimized to achieve the required process temperature range. After that, a regular production cylinder head was disassembled, prepared and the ducts were anodized. With the anodization process conclusion (stage #10) on all four exhaust ducts, the cylinder head was assembled on a working internal combustion engine to be tested on a dynamometer that simulated an actual everyday usage of the engine for approximately 85,000 km[15]. This test was conducted to assure the oxide layer resistance and durability. The oxide layer after the durability test is shown on Figure 15.

The results show an average thickness of 120 µm and an acceptable thickness and structure uniformity that are characteristic of Al-Si alloys anodization, free of cracks and other harmful defects for the component's function. The oxide layers were intact without signs of degradation and spalling, and will provide a suitable surface protection that is the main objective.

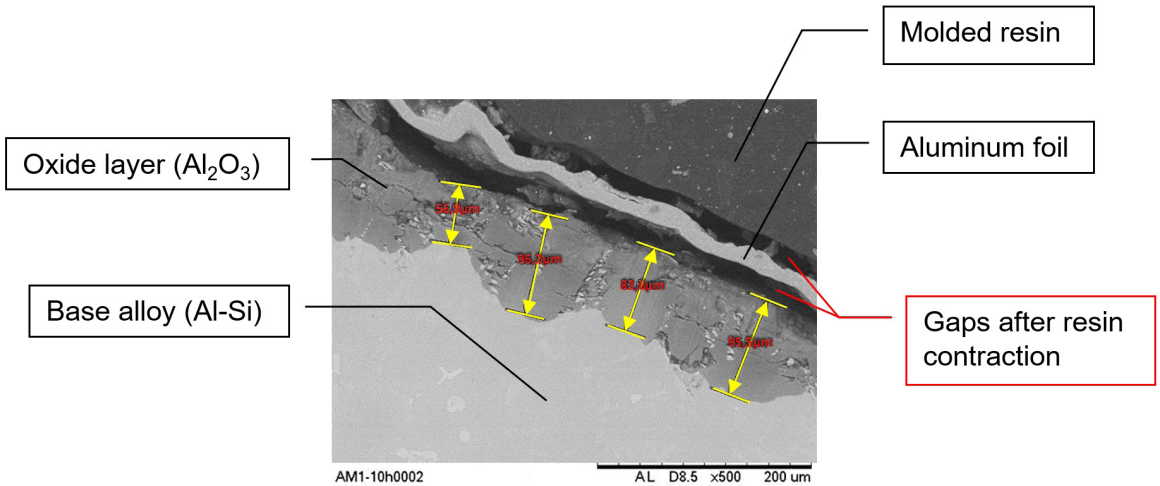

Figure 13. Oxide layer thickness obtained with process parameters of stage #9 showing a cross section of the sample wrapped with an aluminum foil after the inlay process.
Source: author

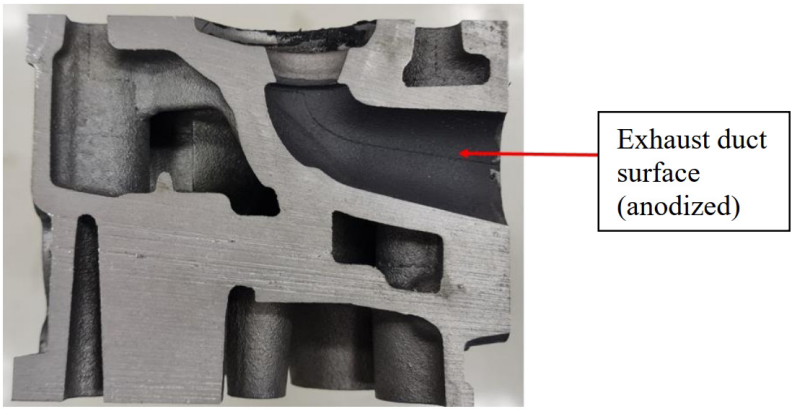

Figure 14. Section of the cylinder head on the exhaust duct showing the internal duct's surface after anodization.
Source: author

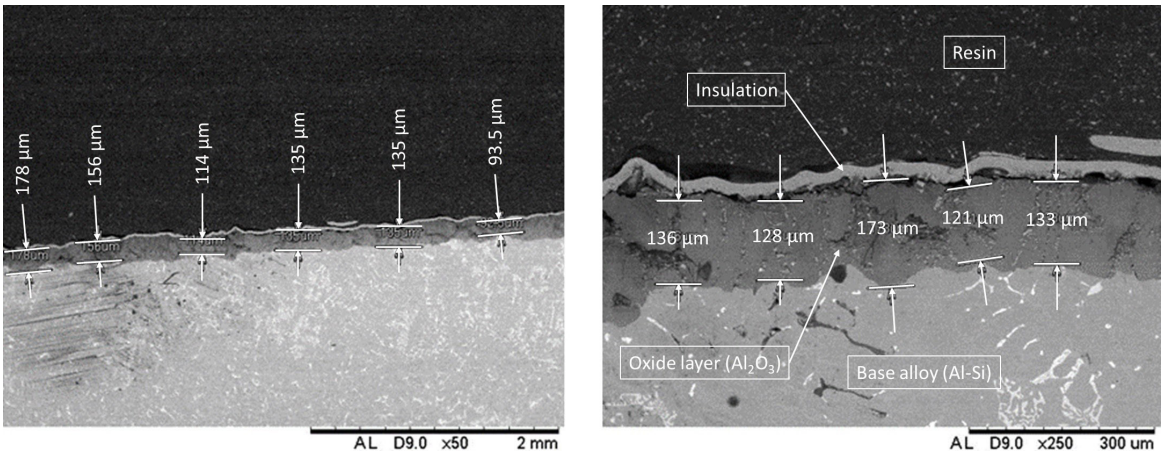

Figure 15. Oxide layer obtained on the ducts' surfaces with process parameters of stage #10, after actual usage test.

4. Conclusion

This research presents the results of an internal surface protection of an internal combustion engine's cylinder head's gases' exhaust ducts. The development of a unique anodization process in which the entire part does not need to be submersed on a container was key to the feasibility of this research's proposal. This drawback was solved with the development of a lean process that performs the anodization only on the required duct's inner surfaces making it economically viable saving resources such as electrolyte volume, cooling capacity and electric power. The oxide layer obtained with this research presents an average thickness of 120 µm with an excellent adhesion to the base aluminum alloy and has shown no degradation after an 85,000 km actual usage test on an internal combustion engine.

5. Acknowledgements

The authors acknowledge the use of the LMM - Laboratory of Microscopy and Microanalysis' facilities of IPEN and to General Motors of Brazil for providing the material and dynamometer test for this research.

6. References

1. Fuoco R, Pinto FBP, Carmezini AS, Fonseca EC. Aluminum based alloy for the production of cylinder heads without heat treatment. Patent application number PI 9901553-6 A2. 1999, May 19. [Portuguese].
2. Brown KR, Venie MS, Woods RA. The increasing use of aluminum in automotive applications. JOM. 1995;47:20-3. http://dx.doi.org/10.1007/BF03221224.
3. Wheeler M, Sheasby P, Kewley D. Aluminum structured vehicle technology - a comprehensive approach to vehicle design and manufacturing in aluminum. Warrendale: SAE International; 1987. [SAE technical paper 870146]. http://dx.doi.org/10.4271/870146.
4. Davis JR. Aluminum and aluminum alloys. In: Davis JR, editor. Alloying: understanding the basics. Materials Park: ASM International; 2001. p. 351-416. http://dx.doi.org/10.1361/autb2001p351.
5. Moreira MF. Cast aluminum alloys: relationship between the cast process and the microstructure [Internet]. São Paulo:

Instituto de Pesquisas Tecnológicas; 2012 [cited 2017 Sep 20]. Available from: http://pmt.usp.br/pmt3402/material/ligas_aluminio_fundidas.pdf. [Portuguese].

6. Tajima S. Anodic oxidation of aluminum. In: Fontana MG, Staehle RW, editors. Advances in corrosion science and technology. Boston: Springer; 1970. p. 229-362. http://dx.doi.org/10.1007/978-1-4615-8252-6_4.
7. Critchlow G, Ashcroft I, Cartwright T, Bahrani D. Anodizing aluminum alloy. United States patent N0.2 US 7,922,889 B2. 2011, Apr 12.
8. Brudzisz A, Brzózka A, Sulka DG. Effect of processing parameters on pore opening and mechanism of voltage pulse detachment of nanoporous anodic alumina. Electrochim Acta. 2015;178:374-84. http://dx.doi.org/10.1016/j.electacta.2015.08.005.
9. Priet B, Odemer G, Blanc C, Giffard K, Arurault L. Effect of new sealing treatments on corrosion fatigue lifetime of anodized 2024 aluminium alloy. Surf Coat Technol. 2016;307(Pt A):206-19. http://dx.doi.org/10.1016/j.surfcoat.2016.07.083.
10. Roshani M, Rouhaghdam AS, Aliofkhazraei M, Astaraee AH. Optimization of mechanical properties for pulsed anodizing of aluminum. Surf Coat Tech. 2017;310:17-24. http://dx.doi.org/10.1016/j.surfcoat.2016.12.046.
11. Zhu B. On the influence of Si on anodising and mechanical properties of cast aluminium alloys. Jönköping: School of Engineering/Jönköping University; 2017.
12. Runge JM. The metallurgy of anodizing aluminum. New York: Springer; 2018.
13. Castro EP, Sillos RM. Alumínio. In: Sillos RM, editor. Technical manual SurTec: surface treatments. 4th ed. São Bernardo do Campo: SurTec do Brasil; 2012 [cited 2016 Oct 6]. p. 229-42. Available from: https://pt.scribd.com/doc/127033749/Manual-Tecnico-2012-Digital. [Portuguese].
14. Araujo JVS, Silva RMP, Klumpp RE, Costa I. The anodizing process of aluminum and its alloys: a historical and electrochemical approach. Quim Nova. 2021;44(8):999-1011. http://dx.doi.org/10.21577/0100-4042.20170748. [Portuguese].
15. Gutierrez H. Private communication. São Caetano do Sul: General Motors do Brasil; 2020.
16. Silva PRC, Colosio MA, Rossi JL. Device, method and process for anodizing the internal surface of exhaust and admission ducts. Patent pending BR 10 2023 012988-9. 2023. [Portuguese]